The 5038-bp fragment was amplified by the polymerase chain reaction (PCR) (Pfu turbo polymerase, Stratagene), sequenced, and inserted into the mammalian expression vector pEGFP.

11. Glutathione S-transferase (GST) fusions of an NR1A fragment (residues 834 to 935) or an NR1C fragment (residues 834 to 898) were incubated for 4 hours at 4°C with HEK 293 cell lysates expressing yotiao. Complexes were isolated by affinity chromatography on glutathione-agarose and were separated by SDS–polyacrylamide gel electrophoresis (PAGE) (4 to 15% gel). Yotiao immunoreactivity was enriched in samples incubated with the GST-NR1A fusion protein but not in samples incubated with the corresponding region of NR1C.
12. HEK 293 cells (10-cm dishes) were transfected with pEGFP (20 μg) or yotiao-GFP (20 μg) by the calcium phosphate method [C. Chen and H. Okayama, *Mol. Cell. Biol.* **7**, 2745 (1987)].
13. The phosphatase blocking peptide consisted of residues 63 to 75 (Gly-Arg-Arg-Val-Ser-Phe-Ala-Asp-Asn-Phe-Gly-Phe-Asn) of the muscle form of the PP1 regulatory G subunit [D. F. Johnson *et al.*, *Eur. J. Biochem.* **239**, 317 (1996)]. This sequence contains the KVXF motif that binds to an allosteric site on PP1C [M. P. Egloff *et al.*, *EMBO J.* **16**, 1876 (1997)].
14. HEK 293 cells plated at low density (~50,000 cells) on 35-mm culture dishes (Falcon) were transfected with 1 μg each of cDNA encoding NR1A, NR2A, CD4 cell surface marker, and yotiao-GFP construct (10 μg) by the calcium phosphate method (*12*). Twenty-four hours after transfection, cells were visually selected by adherence of CD4 antibody–coated beads and GFP epifluorescence. Whole-cell recordings [O. P. Hamill *et al.*, *Pfluegers Arch.* **391**, 85 (1981)] were made with an Axopatch 200B amplifier (Axon Instruments). Patch pipettes (2 to 4 megohms) contained 140 mM Cs methanesulfonate, 10 mM Hepes (pH 7.4), 5 mM adenosine triphosphate (Na salt), 10 mM 1,2-bis(2-aminophenoxy)ethane-*N*,*N*,*N*′,*N*′-tetraacetic acid, and 5 mM $MgCl_2$. Peptides were added to the pipette solution from frozen concentrated stocks. Extracellular solution contained 140 mM NaCl, 5 mM KCl, 1.8 mM $CaCl_2$, 10 mM Na-Hepes (pH 7.4), 10 mM glucose, and 100 μM glycine. Glutamate and cAMP analogs were added from frozen stocks. Rapid solution exchanges were accomplished through a series of flow pipes mounted onto a piezoelectric bimorph to evoke NMDA receptor currents. Cells were lifted off the bottom of the dish to speed the solution exchange time. Currents were digitized at 5 kHz and filtered at 1 kHz with a Digidata 1200B board and Clampex 7 software (Axon Instruments). Series resistance (90 to 95%) and whole-cell capacitance compensation were used. All experiments were done at a holding potential of −60 mV at room temperature. No differences in current amplitudes were detected from control and yotiao-transfected cells (range of 100 pA to 12 nA for both). This variability most likely reflects differences in transfection efficiency. Data are expressed as means ± SEM.
15. J. D. Scott *et al.*, *Proc. Natl. Acad. Sci. U.S.A.* **82**, 4379 (1985).
16. D. W. Carr *et al.*, *J. Biol. Chem.* **267**, 13376 (1992); C. Rosenmund *et al.*, *Nature* **368**, 853 (1994).
17. Desensitization was quantified as the ratio of current remaining at the end of a 500-ms application of glutamate to the peak current. Under our recording conditions, glycine-independent desensitization was the only form of desensitization or inactivation observed [R. A. Lester, G. Tong, C. E. Jahr, *J. Neurosci.* **13**, 1088 (1993); J. J. Krupp, B. Vissel, S. H. Heinemann, G. L. Westbrook, *Mol. Pharmacol.* **50**, 1680 (1996)]. This property of the receptor is regulated by phosphorylation [G. Tong and C. E. Jahr, *J. Neurophysiol.* **72**, 754 (1994)]. Therefore, the extent of desensitization may reflect the phosphorylation state of the receptor or closely associated protein. Non-desensitizing receptors may be highly phosphorylated and less likely to undergo further phosphorylation. Strongly desensitizing currents may arise from largely dephosphorylated receptors, which can then be activated by phosphorylation. Cells that had greater desensitization also had larger increases in current in response to cAMP analogs or Gm peptide.
18. R. S. Westphal, K. A. Anderson, A. R. Means, B. E. Wadzinski, *Science* **280**, 1258 (1998); M. Camps *et al.*, *ibid.*, p. 1262.
19. T. Pawson and J. D. Scott, *ibid.* **278**, 2075 (1997); D. Mochly-Rosen, *ibid.* **268**, 247 (1995).
20. F. Posas and H. Saito, *ibid.* **276**, 1702 (1997); K.-Y. Choi *et al.*, *Cell* **78**, 499 (1994); A. J. Whitmarsh, J. Cavanagh, C. Tournier, J. Yasuda, R. J. Davis, *Science* **281**, 1671 (1998).
21. J. A. Printen, M. J. Brady, A. R. Saltiel, *Science* **275**, 1475 (1997); S. Tsunoda *et al.*, *Nature* **388**, 243 (1997).
22. P. H. Reinhart and I. B. Levitan, *J. Neurosci.* **15**, 4572 (1995); G. F. Wilson, N. S. Magoski, L. K. Kaczmarek, *Proc. Natl. Acad. Sci. U.S.A.* **95**, 10938 (1998).
23. S. M. Lohmann, P. De Camilli, I. Elnig, U. Walter, *Proc. Natl. Acad. Sci. U.S.A.* **81**, 6723 (1984).
24. Rat brain extracts were prepared by Dounce homogenization of frozen brains in phosphate-buffered saline (PBS) containing 1 mM EDTA, 1 mM EGTA, 1 mM 4-(2-aminoethyl)-benzenesulfonyl fluoride, 1 mM benzamidine, pepstatin (2 μg/ml), and leupeptin (2 μg/ml), followed by centrifugation at 40,000*g* for 1 hour. Supernatant (1 ml) was incubated with 20 μl of preimmune or immune serum overnight at 4°C. After addition of protein G–agarose (30 μl) for 1 hour at 4°C, the precipitated complexes were washed five times with homogenization buffer and proteins were eluted with 2× SDS sample buffer. Yotiao was detected by RII overlay. For detection of PKA C subunit activity, immune complexes were incubated with 10 mM cAMP. PKA activity was measured with the substrate Kemptide as described [J. D. Corbin and E. M. Reimann, *Methods Enzymol.* **38**, 287 (1974)]. PKA activity was defined as the activity inhibited by the PKI 5-24 inhibitor peptide (*15*). Immunoprecipitations in Fig. 2 were performed as described [J. Luo *et al.*, *Mol. Pharmacol.* **51**, 79 (1997)].
25. Designated fragments of yotiao were amplified by PCR and subcloned into pGEX-4T3 (Amersham Pharmacia Biotech) or pet30b (Novagen). Inserted sequences were confirmed by DNA sequencing. GST fusion proteins were purified from bacterial extracts by affinity purification with glutathione-agarose (Amersham Pharmacia Biotech).
26. Bacterial extracts expressing fragments of yotiao as histidine-tagged fusion proteins were separated by SDS-PAGE (4 to 15% gels), transferred to polyvinylidene fluoride membranes (Millipore), and blocked overnight in 1% BLOTTO (5% nonfat dry milk, 1% bovine serum albumin, 25 mM tris, and 150 mM NaCl). Blots were then incubated with recombinant PP1 (2 μg/ml) for 2 hours, washed, and incubated with PP1 antisera (1:10,000) for 1 hour. After washing, blots were incubated with horseradish peroxidase–conjugated secondary antibody and washed. PP1 binding was detected by enhanced chemiluminescence (Pierce). Under these conditions PP1 binding is blocked by the Gm peptide, but not by peptides (such as Ht31) that block RII interaction with AKAPs. Protein immunoblots were done as described above with omission of the incubation with recombinant PP1.
27. PP1 activity was determined by incubating recombinant PP1 with substrate for 10 min at 30°C in the absence and presence of a purified HIS-tagged recombinant fragment of yotiao (residues 808 to 1385). Reactions were stopped by addition of trichloroacetic acid. Proteins were precipitated by centrifugation, and liberated ^{32}P was quantitated by Cerenkov counting. Reactions were performed such that the number of counts per minute liberated in the assay was ≤10% of the total cpm of substrate added to each reaction. Dose response curves for yotiao-mediated potentiation of PP1 activity toward phosphorylase *a* showed that the EC_{50} for this enhancement was 52 nM; thus, 500 nM yotiao was used in assays evaluating the effect of yotiao on NR1A dephosphorylation. Phosphorylase *a* was labeled by incubation with phosphorylase kinase; the GST-NR1A fragment was phosphorylated by PKA. Both substrates were labeled in the presence of [γ-^{32}P]ATP and then purified by ammonium sulfate precipitation and fractionation on a D-Salt Excellulose desalting column (Pierce). Labeling of GST alone demonstrated that >80% of the radioactivity was incorporated into the NR1A fragment.
28. We thank V. Coghlan and S. Olsen for isolation and analysis of the original GH4/15 clone; S. Shenolikar, C. Jahr, G. Westbrook, and colleagues at the Vollum Institute for critical evaluation of the manuscript; E. Lee for providing PP1; J. Goldenring for providing a manuscript before publicaton; and A. Westphal, K. Sandstrom, and A. Bishop for expert technical assistance. Supported in part by NIH grants NS10543 (R.S.W.), NS10202 (S.J.T.), GM 48231 (J.D.S.), and NS35050 (M.S.).

23 December 1998; accepted 1 June 1999

A Phospholipase C–Dependent Inositol Polyphosphate Kinase Pathway Required for Efficient Messenger RNA Export

John D. York,[1]* Audrey R. Odom,[1] Robert Murphy,[2] Eric B. Ives,[2] Susan R. Wente[2]*

In order to identify additional factors required for nuclear export of messenger RNA, a genetic screen was conducted with a yeast mutant deficient in a factor Gle1p, which associates with the nuclear pore complex (NPC). The three genes identified encode phospholipase C and two potential inositol polyphosphate kinases. Together, these constitute a signaling pathway from phosphatidylinositol 4,5-bisphosphate to inositol hexakisphosphate (IP_6). The common downstream effects of mutations in each component were deficiencies in IP_6 synthesis and messenger RNA export, indicating a role for IP_6 in *GLE1* function and messenger RNA export.

Spatial and temporal activation of inositol signaling pathways modulates protein machines that enable eukaryotic cells to sense changes in their environment. An essential component within this circuitry is phosphatidylinositol 4,5-bisphosphate (PIP_2), which is hydrolyzed by

Fig. 1. Isolation of genes encoding regulators of mRNA export in a synthetic lethal screen with the *gle1-2 (P380L)* mutant. (**A**) Complementation analysis of *gle1* synthetic lethal alleles. Mutant strains were mated in all pairwise combinations and assayed for nonsectoring diploids, resulting in four groups. Temperature sensitivity was assayed at 37°C. The open reading frame (ORF) that complemented the group is designated as registered with the Stanford Genome Database (SGD); n.d., not determined, as *GSL3* has not been identified. (**B**) Inhibition of nuclear export of poly(A)$^+$ RNA in *gsl1*, *gsl2*, and *gsl3* mutants. In situ hybridization with a digoxigenin-coupled oligo(dT) probe was conducted with wild-type and mutant cells after incubation at 37°C for 1 hour (*22*). Probe localization was detected with a fluorescein isothiocyanate (FITC)–coupled antibody to digoxigenin. Compared to the diffuse cytoplasmic staining in wild-type (WT) cells, marked nuclear accumulation was observed in the mutants. Right panel, coincident DAPI (4′,6′-diamidino-2-phenylindole) staining.

A

Group	No. of alleles	No. of ts alleles	SGD ORF
nup100	9	0	*NUP100*
gsl1	5	0	*YDR315C/IPK1*
gsl2	7	4	*PLC1*
gsl3	3	1	n.d.

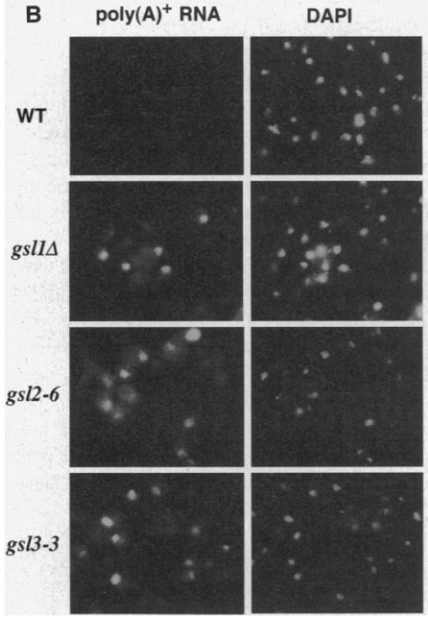

phosphatidylinositol (PI)-specific phospholipase C to produce messenger molecules including inositol 1,4,5-trisphosphate (IP_3) (*1–3*). IP_3 regulates the release of intracellular calcium (*1*), and its modification by multiple dephosphorylation or phosphorylation reactions indicates that IP_3 function may not limited to calcium signaling (*3*, *4*). IP_3 is a precursor to more phosphorylated inositols, such as IP_5 and IP_6, whose signaling functions have not been fully elucidated (*5*).

In eukaryotic cells, transcription and translation are both spatially and temporally segregated by the nuclear envelope (NE). These processes are bridged by the NPC, an essential protein machine that spans the NE and allows the selective nucleocytoplasmic exchange of proteins, RNAs, and ions. Nuclear export of mRNAs requires a series of events: pre-mRNA processing, ribonucleoprotein targeting to the NPC, and energy-dependent translocation through the portal (*6*). The processing and transport of mRNA are tightly linked, such that splicing, polyadenylation, and capping all affect the export process (*7*). Several essential re-

[1]Departments of Pharmacology and Cancer Biology and of Biochemistry, Duke University Medical Center, DUMC 3813, Durham, NC 27710, USA. [2]Department of Cell Biology and Physiology, Box 8228, Washington University School of Medicine, 660 South Euclid, St. Louis, MO 63110, USA.

*To whom correspondence should be addressed. E-mail: yorkj@acpub.duke.edu (J.D.Y.) or swente@cellbio.wustl.edu (S.R.W.)

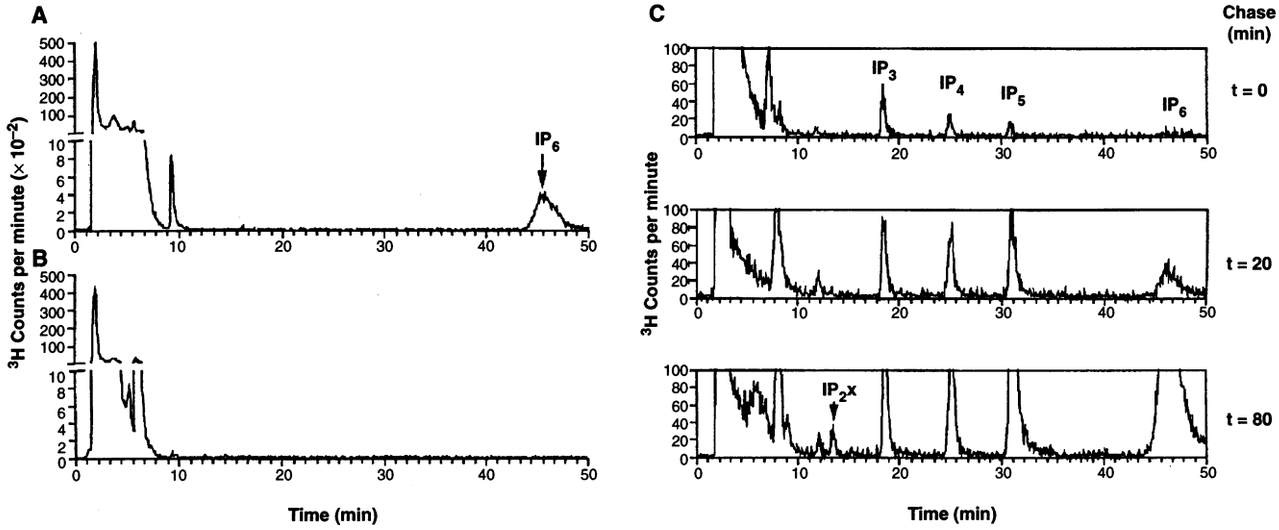

Fig. 2. Requirement of Plc1p for production of IP_6. (A and B) HPLC analysis of soluble extracts prepared after steady-state [^{3}H]inositol labeling of (**A**) wild-type or (**B**) *plc1*Δ yeast strains (*23*). Cells were incubated in complete minimal medium containing [^{3}H]inositol (50 μCi/ml) and harvested during the logarithmic growth phase as described (*23*). Soluble fractions from approximately 5×10^7 cells were resolved by Partisphere strong-anion exchange (SAX) (4.6 mm by 125 mm) HPLC using a linear gradient from 10 mM to 1.7 M ammonium phosphate (pH 3.5) over 25 min, followed by further elution with 1.7 M ammonium phosphate for 25 min. Peaks for inositol (2 min), groPI (4 min), IP_1 (7 to 10 min), and IP_6 (45 min) were detected in wild-type extracts. (**C**) Pulse-chase analysis of cells overexpressing Plc1p. Log phase wild-type cells (1×10^9) harboring a galactose-inducible *PLC1* plasmid (provided by J. Thorner) were grown in complete minimal medium supplemented with 2% raffinose. Expression of Plc1p was induced for 8 hours by addition of galactose (2%) after which 100 μCi/ml [^{3}H]inositol was added for 4 min. Cells were centrifuged, washed, and resuspended in medium supplemented with 1 mM inositol, but with no [^{3}H]inositol. Samples (2×10^8 cells) were taken at the indicated time points, and amounts of soluble inositol phosphates were measured. Individual IP isomers were assigned on the basis of co-elution with known IP standards and sensitivity or resistance to various inositol polyphosphate phosphatase enzymes.

quirements for mRNA export have been identified, including NPC-associated proteins, shuttling heterogenous nuclear ribonucleoprotein (hnRNP) complexes, and the small guanosine triphosphate–binding protein Ran (*8*). Here, we show that phospholipase C and two proteins that influence the generation of IP_6 are required for efficient NPC-mediated export of mRNA.

Gle1p (also known as Rss1p) is an essential NPC-associated factor required for mRNA export in both yeast and human cells (*9*, *10*). To identify additional factors required for Gle1p-mediated export of mRNA, we conducted a genetic screen in the yeast *Saccharomyces cerevisiae* for mutations that were lethal in combination with the temperature-sensitive *gle1-2(P380L)* mutant (*11*). The mutants were classified into four complementation groups (Fig. 1A). Mutations of *GLE1* are synthetically lethal in combination with a *nup100* null allele (*9*), and with mutations in genes encoding various nucleoporins (*12*). Therefore, each complementation group was tested for rescue of the synthetic lethal phenotype with a panel of centromeric plasmids that each expressed a given nucleoporin gene. *NUP100* rescued the largest group; however, none of the plasmids could complement the other three groups. These groups were therefore initially designated *gsl* (for *GLE1* synthetic lethal).

Because Gle1p is specifically required for the export of polyadenylated [poly(A)$^+$] mRNA (*9*, *12*), we used in situ transport assays to test the behavior of the *gsl* mutants. After shift to the restrictive growth temperature, the *gsl1*Δ, *gsl2-6*, and *gsl3-3* mutants all showed an inhibition of poly(A)$^+$ RNA export (Fig. 1B). Over the same time course, no perturbations were observed in nuclear protein import, protein export, or in the morphology of NPCs or the NE (*13*). Thus, the *gsl* mutants are genetically and functionally linked to *GLE1*, and they have specific defects in mRNA export.

The wild-type *GSL1* and *GSL2* genes were identified by complementation of the *gsl1-4* and *gsl2-2* phenotypes with a centromeric yeast genomic library. The minimal complementing DNA fragment for *GSL1* contained an open reading frame (YDR315C) predicted to encode a 33-kD protein. To test whether *GSL1* was required for cell growth, one copy of the gene in a diploid strain was replaced with the kanamycin resistance gene by homologous recombination. Sporulation and dissection of the heterozygous *GSL1/gsl1* null (Δ) strain resulted in the recovery of four viable spores per tetrad. The *gsl1*Δ cells grew similarly to wild-type cells at 23°C, but doubling ceased after 10 hours at 37°C.

The *gsl2* group was complemented by *PLC1*, which encodes the yeast PI-specific phospholipase C that cleaves PIP_2 to produce diacylglycerol and IP_3 (*14*). Cells lacking *PLC1* are viable at 23°C, although they grow slowly, and are inviable at 34°C. To elucidate the role of Plc1p in inositol phosphate (IP) production, we measured the amounts of soluble IPs in wild-type and *plc1*Δ cells by steady-state radiolabeling and high-performance liquid chromatography (HPLC) analysis (Fig. 2). Ino-

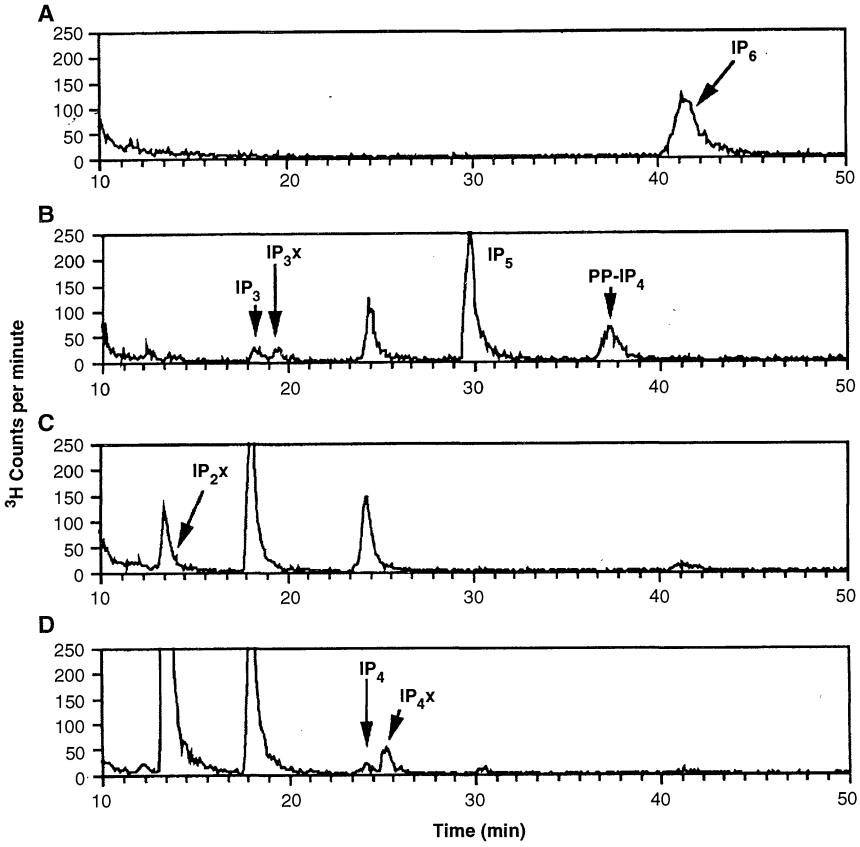

Fig. 3. Requirement of *GSL1* and *GSL3* for production of IP_6. Extracts were prepared from steady-state [^{3}H]inositol-labeled cells and were separated by HPLC (Fig. 2). The cells [(**A**) wild-type, 23°C; (**B**) *gsl1*Δ, 23°C; (**C**) *gsl3-3*, 23°C; and (**D**) *gsl3-3*, 37°C] were labeled over eight doublings at 23°C in complete minimal medium containing 20 μCi of inositol per milliliter and harvested as in Fig. 2. The *gsl3-3* cells (D) were temperature-shifted to 37°C for 6 hours before harvest. Individual IP isomers were assigned as in Fig. 2.

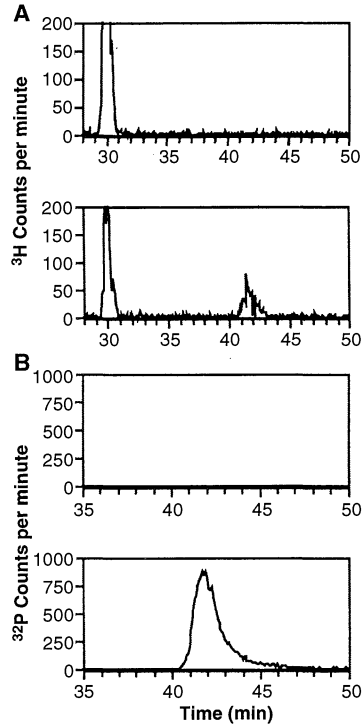

Fig. 4. Intrinsic IP_5 2-kinase activity of Gsl1p/Ipk1p. The coding sequence of *GSL1/IPK1* was fused in frame to glutathione S-transferase (GST), expressed in bacteria, and purified. (**A**) [^{3}H]IP_5 substrate assay. The [^{3}H]IP_5 was purified from *ipk1*Δ cells, and a fraction containing 1500 counts per minute was incubated with either 100 ng of GST only (top) or 1 ng of GST-Ipk1p (bottom) in 50 mM HEPES (pH 7.5), 50 mM NaCl, 10 mM $MgCl_2$, and 2.5 mM adenosine triphosphate at 37°C for 30 min. Reactions were resolved by HPLC (Fig. 2). A conversion of IP_5 to IP_6 of ~40% was observed in GST-Ipk1p reactions. Conversion was time and dose-dependent. (**B**) Assays were done as above in 50 mM Hepes (pH 7.5), 50 mM NaCl, 10 mM $MgCl_2$, 20 μM I(1,3,4,5,6)P_5 (Matreya, Pleasant Gap, Pennsylvania), and 100,000 cpm [γ-^{32}P]ATP at 37°C for 30 min, and separated by HPLC. Approximately 10% of the original radioactivity was converted to [^{32}P]IP_6.

sitol, glycerophosphoinositol (groPI), inositol monophosphate (IP_1), as well as a major peak of IP_6 (representing ~3% of the free inositol), were detected in extracts of wild-type cells (Fig. 2A). In contrast, *plc1*Δ cells fail to produce detectable amounts of IP_6 (Fig. 2B), demonstrating that Plc1p activity is required for its production.

We used a pulse-chase labeling strategy to further define the pathway of Plc1p-dependent IP_6 production in cells overexpressing Plc1p (Fig. 2C). Overproduction of Plc1p resulted in accumulation of multiple inositol polyphosphates. Single major isomers that co-eluted with standards of IP_3, inositol 1,4,5,6-tetrakisphosphate (IP_4), inositol 1,3,4,5,6-pentakisphosphate (IP_5), and IP_6 were observed. At the earliest time point (t = 0 min), amounts of IPs were such that $IP_3 > IP_4 > IP_5 >>> IP_6$. As the chase time progressed, the relative amounts changed such that $IP_3 = IP_4 = IP_5 \geq IP_6$ (t = 20 min), and at later times $IP_6 > IP_5 \gg IP_4 = IP_3$ (t = 80 min). In addition, a bisphosphorylate isomer was detected at later chase times (designated IP_2x because it eluted after inositol 1,4-bisphosphate). At steady-state, cells overexpressing Plc1p had 25 times more IP_6 than wild-type cells, such that the amount of IP_6 was similar to that of free inositol (as above). These results indicate that activation of Plc1p results in the production of IP_3, which appears to be rapidly and sequentially phosphorylated to produce IP_6.

The *gsl1* and *gsl3* strains also failed to produce IP_6 (Fig. 3). Compared to wild-type cells (Fig. 3A), the *gsl1*Δ mutant had increased amounts of IP_3, IP_4, and particularly IP_5, but no detectable IP_6 (Fig. 3B). This mutant had an unidentified IP_3 isomer (IP_3x) and a compound that appeared to be diphosphoinositol tetrakisphosphate ($PP\text{-}IP_4$) because it eluted between IP_5 and IP_6 (*15*). Thus, Gsl1p may be either an IP_5 kinase or a regulator thereof. In contrast, at 23°C, the *gsl3-3* mutant showed a loss of IP_5 and IP_6, and had increased amounts of IP_2x, IP_3, and IP_4 (Fig. 3C). Shifting the *gsl3-3* mutant to 37°C resulted in the disappearance of IP_4, the appearance of an unidentified IP_4 isomer (IP_4x), and increases in the amounts of IP_2x and IP_3 (Fig. 3D). These results indicate a possible block at the IP_4 kinase step with failure to produce IP_5 in *gsl3-3* cells at 23°C. At 37°C, the *gsl3-3* mutation appears to reduce IP_3 kinase activity. The *gsl3-1* mutant grown at 23°C showed a profile similar to that of the *gsl3-3* mutant at 37°C. Thus, Gsl3p may be either a dual-function IP_3 or IP_4 kinase, or a regulator thereof.

To directly test if *GSL1* encodes an intrinsic IP_5-kinase, we analyzed recombinant Gsl1p for activity. Initially, we purified [^{3}H]-labeled IP_5 from radiolabeled *gsl1*Δ cells as a substrate (Fig. 4A). Incubation with recombinant Gsl1p resulted in a specific conversion of IP_5 to IP_6. The IP_5 isomer that accumulates in *gsl1*Δ and in Plc1p-overexpressing cells appears to be inositol 1,3,4,5,6-pentakisphosphate, on the basis of its HPLC elution profile, and this isomer appears to be the precursor to IP_6 in plants, animals, yeast, and slime molds (*3, 16–19*). Recombinant Gsl1p was incubated with [γ-^{32}P]-labeled adenosine triphosphate and pure inositol 1,3,4,5,6-pentakisphosphate. A single [^{32}P]-labeled peak that co-eluted with IP_6 was observed (Fig. 4B). Therefore, Gsl1p is an IP_5 2-kinase, which we designate Ipk1p (for inositol polyphosphate kinase).

To further examine connections between Gle1p and the IP_6 pathway, we conducted genetic suppression analysis (as above). Overexpression of *PLC1* in a temperature-sensitive *gle1-4* mutant rescued growth at 30°C; however rescue was not observed in a *gle1-4* mutant at 37°C or in a *gle1-4 ipk1*Δ background. Overexpression of *GLE1* did not rescue the *gsl2-6/plc1* mutant and resulted in lethality at all temperatures tested. These results support the functional linkage of *GLE1* and *PLC1*, and suggest that IP_6 production is required for the rescue of the *gle1* mutant.

To localize the production of IP_6 in the cell, protein A–tagged Ipk1p was expressed in *ipk1*Δ cells and analyzed by indirect immunofluorescence microscopy (Fig. 5A). Staining for Ipk1p was concentrated in the nucleus and in a punctate pattern at the nuclear periphery that is typical of yeast NPCs and NE. The tagged protein was functionally similar to Ipk1p, and nuclear localization was confirmed by subcellular fractionation analysis (*20*).

Our results indicate a requirement for Plc1p-dependent generation of IP_6 to support mRNA export from the nucleus. Each of the three *gsl* complementation groups correspond to genes that influence IP_6 production. Ipk1p encodes an IP_5 2-kinase whose amino acid sequence shows no similarity to other known inositol kinases. In plants, animals, and yeast, the major route of IP_6 synthesis occurs via such an IP_5 2-kinase (*3, 16–19*). Gsl3p may function as or regulate a dual-function IP_3 or IP_4 kinase similar to an activity purified from budding and fission yeast (*17*). Stimuli that activate IP_6 production may coincidentally enhance mRNA export. IP_6 accumulates under stress conditions (*17*), and Gle1p is required for the export of certain heat-shock mRNAs (*12*). We predict IP_6 acts as a positive regulator of Gle1p-mediated mRNA export. IP_6 may induce conformational changes in the NPC that facilitate translocation of hnRNP complexes (*6*). Alternatively, it may facilitate removal of an export inhibitor (*8*). Precedent exists for direct modulation of protein activity through IP_6 binding; the binding of IP_6 to mammalian synaptotagmin may alter its interaction with the clathrin assembly protein AP2 and thereby inhibit synaptic vesicle trafficking (*21*). NPC proteins, hnRNP components, and Gle1p are candidates for IP_6-binding proteins in the RNA export pathway.

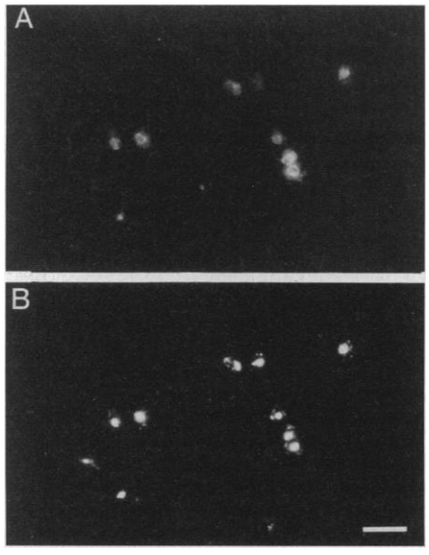

Fig. 5. Localization of Ipk1p at or near the NPC and NE (*20*). (**A**). The intracellular distribution of Ipk1p was determined by indirect immunofluorescence microscopy of yeast *ipk1*Δ cells expressing a protein A–Ipk1p fusion protein (with an NH_2-terminal fusion of the five tandem immunoglobulin G–binding domains from *Staphylococcus aureus* protein A to full-length Ipk1p, on a *LEU2*/2 μ plasmid and under the control of the *GLE1* promoter). Yeast were fixed for 5 min and prepared as described (*22*). Cells were probed with a rabbit anti-mouse antibody (Cappel Laboratories; 1:200 dilution) and with a FITC-conjugated goat anti-rabbit antibody (Cappel Laboratories; 1:200). (**B**) Coincident staining of the nuclei with DAPI. Bar, 5 μm.

References and Notes

1. M. Berridge, *Nature* **361**, 315 (1993).
2. S. B. Lee and S. G. Rhee, *Curr. Opin. Cell Biol.* **7**, 183 (1995).
3. P. W. Majerus, *Annu. Rev. Biochem.* **61**, 225 (1992).
4. R. Irvine, R. Moor, W. Pollock, P. Smith, K. Wreggett, *Philos. Trans. R. Soc. London Ser. B* **320**, 281 (1988).
5. S. Shears, *Biochim. Biophys. Acta* **1436**, 49 (1998).
6. B. Daneholt, *Cell* **88**, 585 (1997).
7. M. S. Lee and P. A. Silver, *Curr. Opin. Genet. Dev.* **7**, 212 (1997); L. E. Maquat, *RNA* **1**, 453 (1995).
8. J. E. Dahlberg and E. Lund, *Curr. Opin. Cell Biol.* **10**, 400 (1998); S. Nakielny and G. Dreyfuss, *ibid.* **9**, 420 (1997); M. Ohno, M. Fornerod, I. W. Mattaj, *Cell* **92**, 327 (1998).
9. R. Murphy and S. Wente, *Nature* **383**, 357 (1996).
10. V. Del Priore, C. A. Snay, A. Bahr, C. N. Cole, *Mol. Biol. Cell* **7**, 1601 (1996); J. L. Watkins, R. Murphy, J. L. T. Emtage, S. R. Wente, *Proc. Natl. Acad. Sci. U.S.A.* **95**, 6779 (1998).
11. To isolate strains harboring *gle1* synthetic lethal mutations, we treated two parental strains with ethylmethane sulfonate to ~25% viability and plated them for growth at 23°C [SWY1791 (*MATα gle1-P380L ade2-1 ade3::HISG ura3-1 his3-11,15 leu2-3,112 TRP1 lys2 can1-100* p*GLE1/ADE3/URA3* p*NUP116/HIS3*) and SWY1792 (*MATa gle1-P380L ade2-1 ade3::HISG ura3-1 his3-11,15 leu2-3,112 trp1-1 LYS2 can1-100* p*GLE1/ADE3/URA3* p*NUP116/HIS3*)]. Approximately 200,000 total colonies were screened using an *ADE3*-dependent color sectoring

assay (*22*). Nonsectoring colonies were isolated, and 28 strains passed tests for dependence on *pGLE1/URA3* and lack of *gle1*Δ alleles. We divided 24 alleles into four complementation groups (Fig. 1A), with 4 remaining unassigned. On the basis of growth defects, the *gsl* alleles were ranked in relative order of increasing severity and penetrance. For characterization experiments, the most severe allele was chosen (for example, *gsl2-6* or *plc1*Δ, *gsl1*Δ, *gsl3-3*, *gle1-4*). Exceptions include the synthetic lethal screen (*gle1-2*) and cloning of *GSL* genes (*gsl1-4*, *gsl2-2*), in which cases the allele used was that most readily complemented by *GLE1* in a colony sectoring assay. Allele-specific differences were noted in the IP profiles of *gsl3-1* and *gsl3-3*, and likely represent distinct mutations.

12. C. A. Saavedra, C. M. Hammell, C. V. Heath, C. N. Cole, *Genes Dev.* **11**, 2845 (1997); F. Stutz *et al.*, *ibid.*, p. 2857.
13. The *plc1* mutant (*gsl2-6*) was also assayed over a time course for poly(A)$^+$ RNA export, and accumulation in some cells was detectable beginning 15 to 30 min after the shift to 37°C. Nuclear protein export was assayed using a green fluorescent protein (GFP) tagged with nuclear localization and export sequences [K. Stade, C. S. Ford, C. Guthrie, K. Weis, *Cell* **90**, 1041 (1997)]. Import assays were performed with a nuclear localization sequence–GFP reporter [N. Shulga *et al.*, *J. Cell Biol.* **135**, 329 (1996)]. Thin-section electron microscopy was performed as described [S. R. Wente and G. Blobel, *ibid.* **123**, 275 (1993)].
14. J. S. Flick and J. Thorner, *Mol. Cell. Biol.* **13**, 5861 (1993).
15. S. Safrany and S. Shears, *EMBO J.* **17**, 1710 (1998).
16. B. Phillippy, A. Ullah, K. Ehrlich, *J. Biol. Chem.* **269**, 28693 (1994).
17. P. Ongusaha, P. Hughes, J. Davey, R. Mitchell, *Biochem. J.* **335**, 671 (1998); F. Estevez, D. Pulford, M. Stark, A. Carter, C. Downes, *ibid.* **302**, 709 (1994).
18. L. Stephens and R. Irvine, *Nature* **326**, 580 (1990).
19. B. Drobak, *Biochem. J.* **288**, 697 (1992); F. Menniti, K. Oliver, J. Putney, S. Shears, *Trends Biochem. Sci.* **18**, 53 (1993).
20. Expression of protein A–tagged Ipk1p on a 2 μm plasmid (with the *GLE1* promoter) complements the synthetic lethality of *gsl1-4 gle1-2* cells and rescues production of IP_6 in *gsl1*Δ cells. Protein A–Ipk1p was not visible when expressed on a centromere plasmid or integrated. In subcellular fractionation experiments, the majority of the centromere expressed protein A–Ipk1p was isolated with nuclei, suggesting the results in Fig. 5 reflect that of endogenous Ipk1p.
21. S. M. Voglmaier *et al.*, *Biochem. Biophys. Res. Commun.* **187**, 158 (1992).
22. R. Murphy, J. L. Watkins, S. R. Wente, *Mol. Biol. Cell* **7**, 1921 (1996).
23. L. E. Stolz, W. J. Kuo, J. Longchamps, M. K. Sekhon, J. D. York, *J. Biol. Chem.* **273**, 11852 (1998).
24. We thank J. Datto for technical help, J. Thorner for sharing unpublished data, and K. Weis and D. Goldfarb for plasmids. Supported by a Burroughs Wellcome Fund Career Award in the Biomedical Sciences (J.D.Y.), a Whitehead Scholar Award (J.D.Y.), Duke University Medical Scientist Training Program (A.R.O.), an NIH Training Grant for predoctoral trainees (R.M. and E.B.I.), and grants from the American Cancer Society (Junior Faculty Research Award) (S.R.W.) and the National Institutes of General Medical Science (S.R.W.).

8 February 1999; accepted 27 May 1999

The Cavity and Pore Helices in the KcsA K^+ Channel: Electrostatic Stabilization of Monovalent Cations

Benoît Roux[1] and Roderick MacKinnon[2]

The electrostatic influence of the central cavity and pore alpha helices in the potassium ion channel from *Streptomyces lividans* (KcsA K^+ channel) was analyzed by solving the finite difference Poisson equation. The cavity and helices overcome the destabilizing influence of the membrane and stabilize a cation at the membrane center. The electrostatic effect of the pore helices is large compared to that described for water-soluble proteins because of the low dielectric membrane environment. The combined contributions of the ion self-energy and the helix electrostatic field give rise to selectivity for monovalent cations in the water-filled cavity. Thus, the K^+ channel uses simple electrostatic principles to solve the fundamental problem of ion destabilization by the cell membrane lipid bilayer.

The cell membrane presents a large energy barrier to ion permeation. Known as the dielectric barrier, this impediment to ion passage is a fundamental property of the low electrical polarizability of the membrane hydrocarbon (*1*). The structure determination of the KcsA K^+ channel shows two unexpected features of its ion conduction pore (*2*). First, at the level of the bilayer center, the pore forms a cavity large enough to contain around 50 water molecules (~5 Å radius), and second, four α helices (pore helices) point their COOH-termini at the cavity center (Fig. 1). It has been proposed that the water-filled cavity and oriented pore helices are the structural basis by which the K^+ channel overcomes the dielectric barrier (*2*).

The K^+ channel not only lowers the dielectric barrier, but it stabilizes a cation near the bilayer center. This conclusion is based on difference Fourier analysis of ion-substituted crystals. When K^+ was substituted with the more electron-dense Rb^+, resulting difference maps showed a positive peak at the cavity center (Fig. 1; red mesh). Further, if the less electron-dense Na^+ is used to substitute K^+, a negative peak is observed (Fig. 1; green mesh). We thus conclude that the cavity is occupied by a cation. In the present theoretical analysis, we investigated whether the cavity and pore helices are sufficient to overcome the dielectric barrier and account for the presence of a cation at the bilayer center.

The electrostatic stabilization of an ion by a water-filled cavity at the membrane center can be understood through a calculation based on the Born theory of solvation (*3*). The free energy for transferring an ion from bulk water into a cavity of radius R and dielectric constant ε_w embedded in a medium of low dielectric constant ε_m is given by

$$\Delta G = (1/2)(Q^2/R)(1/\varepsilon_m - 1/\varepsilon_w) \qquad (1)$$

This equation yields a value of 16.2 kcal/mol for the transfer of K^+ from aqueous solution to a 5 Å (radius) water-filled sphere (ε_w = 80) surrounded by hydrocarbons (ε_m = 2). Transferring the ion from water directly into hydrocarbon (no cavity) would have an energetic cost of more than 60 kcal/mol, and so the cavity will stabilize the ion by more than 40 kcal/mol.

The remaining 16.2 kcal/mol still represents a large energy barrier that precludes the presence of an ion in the cavity. Can the pore helices account for the additional stabilization through the electrostatic field that they impose on their environment (*2, 4*)? According to accepted principles, there are two arguments against this idea. First, the nearest carbonyl oxygen at the COOH-terminus of the helices (Thr^{74}) is 8 Å from the cavity center, whereas electrostatic effects due to α helices are thought to be very small and short range (*5*). Second, the cavity contains about 50 water molecules that would be expected to shield the electric field of the α helix. An α helix in water barely interacts (~−0.14 kcal/mol) with a monovalent cation located 8 Å from its COOH-terminus.

To address the basis of ion stabilization at the center of the KcsA K^+ channel, it is necessary to account for the dielectric shielding in the complex membrane environment. We calculated the electrostatic free energy of a K^+ ion in the center of the cavity, using a macroscopic continuum model of the environment surrounding the KcsA K^+ channel protein. The channel was represented in full atomic detail with all explicit partial charges, whereas the membrane was assigned a dielectric constant of 2 and the water, including the pore and cavity, was assigned a value of 80 (*6*).

[1]GRTM, Dipartements de Physique et Chimie, Université de Montréal, Case Postal 6128, succursale Centre-Ville, Montréal, Canada H3C 3J7. [2]Howard Hughes Medical Institute, Laboratory of Molecular Neurobiology and Biophysics, Rockefeller University, 1230 York Avenue, New York, NY 10021, USA.